Analysis of multilayer rotor induction motor with higher space harmonics taken into account

Prof. J.F. Gieras, PhD

Indexing terms: Induction motors, Electromagnetic theory

Abstract: The paper presents a consistent electromagnetic theory of a multilayer rotor induction motor with distributed parameters. Equations describing the two-dimensional field distribution in the rotor have been used to obtain recurrence relations for the resultant rotor impedance. These relations include the higher space harmonics produced by the stator MMF curve. The classical T configuration equivalent circuit has been extended and adjusted to model a multilayer rotor. Positive- and negative-sequence currents have been taken into account and impedances for forward- and backward-travelling field have been found.

The method of the performance calculation for a multilayer rotor induction motor, including current assymetry and higher space harmonics, has been worked out. The approach presented may be helpful in the analysis and synthesis of induction machinery with specially constructed rotors (secondaries). The existing theory has been developed and generalised.

List of principal symbols

A = stator line current density
a = $\exp(2j\pi/3)$
a_{Ri}, a_{xi} = coefficients for resistance and reactance, taking into account magnetic permeability and hysteresis losses, respectively
B = magnetic flux density
d = thickness of high conductivity layer
E = electric field strength, peak value; EMF, RMS value
F = force
f = frequency
g = airgap
H = magnetic field strength, peak value
h_{Fe} = thickness of solid ferromagnetic core
I = electric current
k_C = Carter coefficient
$k_{te\nu}$ = Russell and Norsworthy factor for νth harmonic
k_{sat} = saturation factor of magnetic circuit
$k_{tr\nu}$ = impedance turns ratio for νth harmonic
k_{w1} = primary winding factor
$k_{z\nu i}$ = impedance increase factor due to edge effect
L_i = length of the stator core (in y-direction)
m_1 = number of stator phases
N_1 = number of stator turns per phase
n = speed in rev/s
P_g = airgap (electromagnetic) power
p = number of pole pairs
R = resistance
s = slip
T = torque
t_{ov} = thickness of high conductivity layer behind ferromagnetic core
v = linear velocity in m/s
w = length of rotor core (in y-direction)
w_{ov} = length of high conductivity layer behind ferromagnetic core (overhang)
X = reactance
Z = impedance
z = surface wave impedance
α = complex propagation constant independent of pole pitch
β = real constant, phase angle
κ = complex propagation constant dependent on pole pitch
μ_i = magnetic permeability (μ_0 = permeabiity of free space, μ_{rsi} = relative surface permeability)
ν = space harmonic of field distribution along pole pitch
σ_i = electric conductivity
τ = pole pitch
ω = $2\pi f$ = angular frequency

Subscripts

c = common
Cu = copper (high conductivity layer)
d = developed
dif = differential leakage
Fe = steel (ferromagnetic)
g = airgap
i = $1, 2, \ldots, k-1, k$ = ith layer
in = input
L = load
o = characteristic impedance
s = synchronous
t = total (resultant)
ν = νth space harmonic
1 = stator
2 = rotor

Superscripts

$(i = 1, 2, \ldots, k-1, k)$ = number of layers of which the considered machine consists
primed = value referred to the stator
$+$ = positive-sequence (forward-travelling)
$-$ = negative-sequence (backward-travelling)

Paper 7413B (P1), first received 19th April 1989 and in revised form 17th April 1990

The author is with the Department of Electrical Machines and Drives, Academy of Technology and Agriculture, Al. S. Kaliskiego 7, 85-763 Bydgoszcz, Poland

1 Introduction

A general theory of electromechanical energy conversion can be derived from the electromagnetic field theory. The field theory enables us, in a straightforward way, to obtain equivalent impedances and to develop an equivalent circuit for induction machines with distributed parameters. Investigations in electromechanics, including some recent work, are oriented towards modelling induction machines on the basis of the multilayer theory derived directly from the Maxwell field equations.

Devices and problems that can be modelled in this way include induction motors with solid rotors, linear induction machines, induction pumps for liquid metals, eddy current couplings and brakes, electrodynamic and electromagnetic levitation systems, screens in superconducting generators, nonmagnetic thin-cylinder induction motors, screened rotor induction motors, induction-type instruments etc.

The idea of a one-dimensional multilayer theory was first introduced by Pipes [1], who obtained general formulas for the elements of a transfer matrix for any region. Greig and Freeman [2–6] expanded the Pipes multilayer theory [1] and Cullen and Barton's transmission line theory [7] to deduce an equivalent circuit for induction machines and low frequency induction devices. Each layer was replaced by a T equivalent circuit and the equivalent circuits for adjacent regions were connected in tandem. The impedances that constituted the T equivalent circuit of a particular region, were calculated from the physical parameters of that region alone. Transfer matrices were utilised in further work, e.g. References 8 and 9. Other approaches to the analysis of stratified media are discussed in many papers [8, 10–16]

The main intention of this paper is to present a new method of analysis for induction machines with distributed parameters, including space harmonics by combining field and circuit theory. Any type of induction machine can be modelled by a T equivalent circuit in which the rotor (secondary) impedance and self-inductance reactance are obtained from electromagnetic field theory. In the multilayer model presented here, the normal limitations imposed by the amount of algebraic manipulation involved are removed by the use of recurrence relations [13–15].

2 Formulation of the problem

The model of an induction machine with distributed parameters (Fig. 1) consists of an arbitrary number of layers $i = k$, where the first layer $i = 1$ is a halfspace. The numbers $i > 1$ correspond to successive layers with finite thicknesses. It is assumed that the regions are planar, the curvature of rotary machines is neglected, the anisotropy is ignored, the electric currents flow only in the x- and y-directions and that the displacement currents are considered negligible. The current sheet, infinitely thin in the z-direction, and the magnetic flux density in the airgap vary sinusoidally in the x- and z-directions, and with the time. Each of the layers can be made of an arbitrary material, characterised by its magnetic and electric properties.

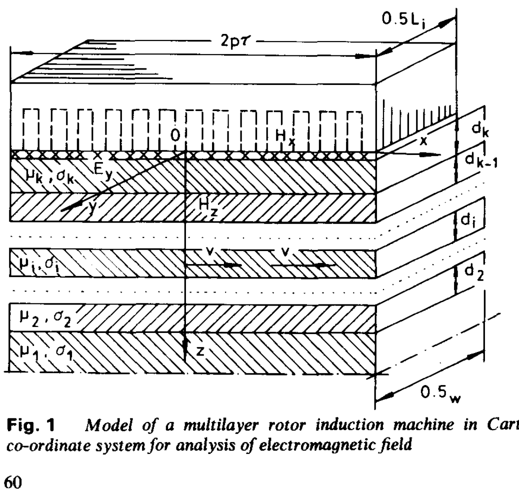

Fig. 1 *Model of a multilayer rotor induction machine in Cartesian co-ordinate system for analysis of electromagnetic field*

The two-dimensional electromagnetic field distribution satisfies the Laplace equation in the ith nonconductive layer (air)

$$\nabla^2 H_{vi}^{(k)} = 0 \quad \nabla^2 E_{vi}^{(k)} = 0 \tag{1}$$

and Helmholtz equation in the ith conductive layer

$$\nabla^2 H_{vi}^{(k)} = \alpha_{vi}^2 H_{vi}^{(k)} \quad \nabla^2 E_{vi}^{(k)} = \alpha_{vi}^2 E_{vi}^{(k)} \tag{2}$$

in which the complex propagation constant for the vth space harmonic is

$$\alpha_{vi} = (1 + j)(0.5\, \omega s_{vi} \mu_i \sigma_i')^{1/2} \tag{3}$$

The slip s_{vi} corresponding to the vth harmonic of the stator MMF is

(i) for the forward-travelling magnetic field

$$s_{vi}^+ = 1 - v(1 - s_i) \tag{4a}$$

(ii) for the backward-travelling magnetic field

$$s_{vi}^- = 1 + v(1 - s_i) \tag{4b}$$

where the slip s_i corresponds to the fundamental harmonic.

Magnetic properties of the layers are characterised by the complex magnetic permeability [17]:

$$\mu_i = \mu_0 \mu_{rsi} (\mu_i' - \mu_i'') \tag{5}$$

where μ_{rsi} = relative surface permeability and μ_0 = permeability of free space. For both paramagnetic and diamagnetic layers $\mu_i' = 1$ and $\mu_i'' = 0$. For ferromagnetic layers

$$\mu_i' = a_{Ri} a_{Xi} \quad \mu_i'' = 0.5(a_{Ri}^2 - a_{Xi}^2) \tag{6}$$

The coefficients a_{Ri} and a_{Xi} take into account magnetic saturation and hysteresis [17]. Variation of magnetic permeability along the z-axis only is included.

The equivalent electric conductivity

$$\sigma_i' = k_{te} \sigma_i \tag{7}$$

includes so called 'transverse edge effects'. The coefficient $k_{te} < 1$ of transverse edge effects has been derived amongst others by Russell and Norsworthy [18].

The general solution for eqns. 1 and 2 has the following Fourier series form:

(i) For the forward-travelling field

$$F_i^{(k)+}(x, z, t) = \sum_{v=1}^{\infty} F_{vi}^{(k)+}(x, z, t) = \sum_{v=1}^{\infty} e^{j(\omega s_{vi} t - \beta_v x)} \times [C_{1vi}^{(k)} C_{3vi}^{(k)} e^{-\kappa_{vi} z} + C_{1vi}^{(k)} C_{4vi}^{(k)} e^{\kappa_{vi} z}] \tag{8a}$$

(ii) For the backward-travelling field

$$F_i^{(k)-}(x, z, t) = \sum_{v=1}^{\infty} F_{vi}^{(k)-}(x, z, t) = \sum_{v=1}^{\infty} e^{j(\omega s_{vi} t + \beta_v x)} \times [C_{2vi}^{(k)} C_{3vi}^{(k)} e^{-\chi_{vi} z} + C_{2vi}^{(\kappa)} C_{4vi}^{(\kappa)} e^{\chi_{vi} z}] \quad (8b)$$

where $F_i^{(k)}$ = scalar projections of $H_i^{(k)}$ or $E_i^{(k)}$ vectors parallel to the x-, y- and z-axes, respectively, and C_{1vi}, C_{2vi}, C_{3vi}, C_{4vi} = complex constants.

The complex propagation constant, dependent on the pole pitch τ, is

$$\kappa_{vi} = (\alpha_{vi} + \beta_v)^{1/2} \quad (9)$$

in which

$$\beta_v = v\pi/\tau \quad (10)$$

The electric field components $E_{zvi}^{(k)} = 0$ since the currents flow only in the x- and y-directions. For $z \to \infty$, the field must vanish, so that for $i = 1$ (first layer) $C_{1vi}^{(k)} C_{4vi}^{(k)} = C_{2v1}^{(k)} C_{4v1}^{(k)} = 0$. The remaining constants $C_{1vi}^{(k)}$, $C_{2vi}^{(k)}$, $C_{3vi}^{(k)}$ and $C_{4vi}^{(k)}$ can be evaluated from the conditions $\nabla \cdot \boldsymbol{B}_{vi}^{(k)} = 0$, $\nabla \times \boldsymbol{E}_{vi}^{(k)} = j\omega s_{vi} \mu_i \boldsymbol{H}_{vi}^{(k)}$, from boundary conditions between the layers and from boundary conditions between the last layer $i = k$ and the stator (primary) ferromagnetic core (Appendix 9.1). In this way the final solution for eqns. 1 and 2 can be obtained. It expresses the distribution of a 2D electromagnetic field in a multilayer structure and is given in References 13–15 as a set of recurrence relations.

The unit impedance of a multilayer rotor (secondary), as shown in Fig. 1, is expressed as a ratio of tangential electric to magnetic components at $z = 0$, i.e.

$$z_{vk}^{(k)} = \left[\frac{E_{yvk}^{(k)}}{H_{xvk}^{(k)}}\right]_{z=0} = \left[\frac{z_{vk}^{(k)}}{z_{vk-1}^{(k-1)}}\right]\left[\frac{z_{vk-1}^{(k-1)}}{z_{vk-2}^{(k-2)}}\right] \cdots \left[\frac{z_{vi}^{(i)}}{z_{vi-1}^{(i-1)}}\right] \cdots \left[\frac{z_{v3}^{(3)}}{z_{v2}^{(2)}}\right] z_{v1}^{(1)} \quad (11)$$

where

$$\frac{z_{vi}^{(i)}}{z_{vi-1}^{(i-1)}} = \frac{j\omega_{vi}\mu_i}{\kappa_{vi}} \frac{\dfrac{\omega_{vi}}{\omega_{vi-1}} \dfrac{1}{\tanh(\kappa_{vi} d_i)} + \dfrac{j\omega_{vi}\mu_i}{\kappa_{vi}} \dfrac{1}{z_{vi-1}^{(i-1)}}}{\dfrac{j\omega_{vi}\mu_i}{\kappa_{vi}} \dfrac{1}{\tanh(\kappa_{vi} d_i)} + \dfrac{\omega_{vi}}{\omega_{vi-1}} z_{vi-1}^{(i-1)}} \quad (12a)$$

or

$$z_{vi}^{(i)} = \frac{j\omega_{vi}\mu_i}{\kappa_{vi}} \frac{\dfrac{\omega_{vi}}{\omega_{vi-1}} z_{vi-1}^{(i-1)} \dfrac{1}{\tanh(\kappa_{vi} d_i)} + \dfrac{j\omega_{vi}\mu_i}{\kappa_{vi}}}{\dfrac{j\omega_{vi}\mu_i}{\kappa_{vi}} \dfrac{1}{\tanh(\kappa_{vi} d_i)} + \dfrac{\omega_{vi}}{\omega_{vi-1}} z_{vi-1}^{(i-1)}} \quad (12b)$$

and

$$z_1^{(1)} = j\omega_{v1}\mu_1/\kappa_{v1} \quad (13)$$

Eqn. 12b is similar to that expressing the input impedance of a transmission line (Appendix 9.2). Eqn. 13 relates to a model consisting of one layer of infinite thickness ($i = 1$).

3 Impedance of multilayer rotor (secondary)

By analogy to an open-circuited line (Appendix 9.2), the unit impedance z_{vi} of a single layer with finite thickness d_i can be found as a limit of $z_{vi}^{(i)}$ when $(\omega_{vi}/\omega_{vi-1}) z_{vi-1}^{(i-1)} \to \infty$, i.e.

$$z_{vi} = \frac{j\omega_{vi}\mu_i}{\kappa_{vi}} \frac{1}{\tanh(\kappa_{vi} d_i)} \quad (14)$$

Hence, eqn. 12b takes on a similar form to eqn. 47 and can be rewritten in the form

$$z_{vi}^{(i)} = \frac{z_{vi} \dfrac{\omega_{vi}}{\omega_{vi-1}} z_{vi-1}^{(i-1)} + \left(\dfrac{j\omega_{vi}\mu_i}{\kappa_{vi}}\right)^2}{z_{vi} + \dfrac{\omega_{vi}}{\omega_{vi-1}} z_{vi-1}^{(i-1)}} \quad (15)$$

It is not difficult to see that the impedance

$$z_{vci} = \left(\frac{j\omega_{vi}\mu_i}{\kappa_{vi}}\right) \frac{1}{z_{vi} + \dfrac{\omega_{vi}}{\omega_{vi-1}} z_{vi-1}^{(i-1)}} \quad (16)$$

is connected in series with z_{vi} and in parallel with $(\omega_{vi}/\omega_{vi-1}) z_{vi-1}^{(i-1)}$. The impedance z_{vi}, given by eqn. 14, is a unit impedance of the ith layer with thickness d_i, whereas z_{vi} according to eqn. 15 is a resultant unit impedance of the layers 1, 2, …, i. The first layer, with its unit impedance $z_{v1} = z_{v1}^{(1)}$, is a halfspace.

In a multilayer rotor induction machine a solid ferromagnetic yoke or shaft can be regarded as a halfspace with unit impedance z_{v1}. In a multilayer secondary single-sided linear induction machine, an air half space for which $\kappa_{v1} = \beta_v$ is regarded as the first layer ($i = 1$) with unit impedance z_{v1} and unit resistance $r_{v1} \to \infty$. The first layer is motionless. The second layer ($i = 2$) belongs to the secondary, which moves with slip $s_v = s_{vi}$ relative to the primary magnetic travelling field. Thus, $\omega_{v2} = s_v \omega = s_v \omega_1$. For $z_{v1} \to \infty$, the unit impedance of a single-sided linear induction motor is

$$z_{v2}^{(2)} = z_{v2} = \frac{j\omega_{v2}\mu_2}{\kappa_{v2}} \frac{1}{\tanh(\kappa_{v2} d_2)} \quad (17)$$

In any induction machine, the last layer $i = k$ is the airgap, for which $\kappa_{vk} = \beta_v$, $\mu_k = \mu_0$, $d_k = k_C k_{sat} g$ and $s_v \omega_{vk} = s_v \omega = \omega_{vk-1}$. The real airgap g has to be multiplied by the Carter factor $k_c \geq 1$ and the saturation factor $k_{sat} \geqq 1$ of the magnetic circuit. Thus

$$z_{vk}^{(k)} = \left(\frac{j\omega_{vk}\mu_0}{\beta_v}\right)^2 \frac{1}{z_{vk} + \dfrac{1}{s_v} z_{vk-1}^{(k-1)}} + \frac{\dfrac{1}{s_v} z_{vk-1}^{(k-1)} z_{vk}}{\dfrac{1}{s_v} z_{vk-1}^{(k-1)} + z_{vk}} \quad (18)$$

and

$$z_{vk} = \frac{j\omega\mu_0\tau}{v\pi} \frac{1}{\tanh\left(v \dfrac{\pi}{\tau} k_C k_{sat} g\right)} \simeq j \frac{2\mu_0 f\tau^2}{v^2 \pi k_c k_{sat} g} \quad (19)$$

The other layers $2 \leq i \leq k - 1$ usually run with the slip s_v relative to the flux crossing the airgap and $\omega_{vk-1} = \omega_{vk-2} = \cdots = \omega_{v2}$.

If the length of the rotor (secondary in the y-direction is L_i, the pole pitch is τ an the impedance turns ratio is

$$k_{trv} = 2m_1(N_1 k_{w1v})^2/vp \quad (20)$$

the impedances (eqn. 15) referred to the stator (primary) are as follows:

$$Z'^{(k)}_{vk}(s_v) = \frac{\left(\frac{j\omega\mu_0}{\beta_v}\right)^2 \left(v\,\frac{L_i}{\tau}\right)^2 k^2_{trv}}{Z'_{vk} + \frac{1}{s_v}\,Z'^{(k-1)}_{vk-1}(s_v)} + \frac{\frac{1}{s_v}\,Z'^{(k-1)}_{vk-1}(s_v) Z'_{vk}}{\frac{1}{s_v}\,Z'^{(k-1)}_{vk-1}(s_v) + Z'_{vk}}$$

$$Z'^{(k-1)}_{vk-1}(s_v) = \frac{\left(\frac{js_v\,\omega\mu_{k-1}}{\kappa_{vk-1}}\right)^2 \left(v\,\frac{L_i}{\tau}\right)^2 k^2_{trv}}{Z'_{vk-1}(s_v) + Z'^{(k-2)}_{vk-2}(s_v)} + \frac{Z'^{(k-2)}_{vk-2}(s_v) Z'_{vk-1}(s_v)}{Z'^{(k-2)}_{vk-2}(s_v) + Z'_{vk-1}(s_v)} \tag{21}$$

....

$$Z'^{(i)}_{vi}(s_v) = \frac{\left(\frac{js_v\,\omega\mu_i}{\kappa_{vi}}\right)^2 \left(\frac{L_i}{\tau}\right)^2 k^2_{trv}}{Z'_{vi}(s_v) + Z'^{(i-1)}_{vi-1}(s_v)} + \frac{Z'^{(i-1)}_{vi-1}(s_v) Z'_{vi}(s_v)}{Z'^{(i-1)}_{vi-1}(s_v) + Z'_{vi}(s_v)}$$

....

$$Z'^{(2)}_{v2}(s_v) = 0 + Z'_{v2}(s_v)$$

The primed variable means that the impedance $Z'^{(i)}_{vi}(s_v)$ is referred to the stator (primary) winding, i.e. $Z'^{(i)}_{vi}(s_v) = k_{trv} Z^{(i)}_{vi}(s_v)$.

Eqns. 19–21 yield the airgap impedance referred to the stator (primary) in a similar form to that in the classical theory of induction machines, i.e.

$$Z'_{vk} = k_{trv}\, z_{vk}\, v\,\frac{L_i}{\tau} \simeq jX_{gv} = j4m_1\mu_0 f\,\frac{(N_1 k_{w1})^2}{v^2 \pi p}\,\frac{L_i \tau}{k_C\, k_{sat}\, g} \tag{22}$$

The impedance (eqn. 22) is independent of the slip s_v and holds only the imaginary part x_{gv}. For $v = 1$ the above equation yields the self-inductance reactance, i.e.

$$X_g = 4m_1\mu_0 f\,\frac{(N_1 k_{w1})^2}{p}\,\frac{L_i \tau}{k_C\, k_{sat}\, g} \tag{23}$$

where k_{w1} = winding factor for the fundamental harmonic. For $v > 1$, eqn. 20 yields the differential leakage inductive reactance:

$$X_{1dif} = \sum_{v>1} X_{gv} = \frac{1}{k^2_{w1}}\, X_g \sum_{v>1} \left(\frac{k_{w1v}}{v}\right) \tag{24}$$

The impedances of the layers from $i = 2$ to $i = k - 1$, referred to the stator (primary), have the following general form:

$$Z'_{vi}(s_v) = k_{trv}\, z_{vi}\, v\,\frac{L_i}{\tau} = \frac{js_v\,\omega\mu_i}{\kappa_{vi}}\,\frac{1}{\tanh(\kappa_{vi} d_i)}\,k_{trv}\, v\,\frac{L_i}{\tau} \tag{25}$$

To take into account transverse edge effects, either eqn. 7 or the impedance increase coefficient $k_{zvi} > 1$ can be used. In the second case, the impedances (eqn. 25) should be multiplied by

$$k_{zvi} = 1 + 0.5\,\frac{\tau}{v^2 L_i} \tag{26}$$

The coefficient k_{zvi} can also take other forms, Reference 19. The author recommends the equivalent electric conductivity (eqn. 7) for nonmagnetic layers and the coefficient (eqn. 26) for ferromagnetic layers.

Appendix 9.3 contains an example how to estimate the rotor impedance.

If we let $s_v = s_v^+$, the impedance $Z'^{+}_{vi}(s_v^+)$ corresponds to the forward-travelling field (positive sequence currents) and if $s_v = s_v^-$, the impedance $Z'^{-}_{vi}(s_v^-)$ corresponds to the backward-travelling field (negative sequence currents).

4 Equivalent circuit

All the impedances expressed by the formula

$$Z'_{vci} = k^2_{trv}\, z_{vci}\left(v\,\frac{L_i}{\tau}\right)^2 \tag{27}$$

where z_{vci} is given by eqn. 16, should be regarded as so-called 'common impedances' of the ith layer and the layers from $i - 1$ to $i = 2$. This is an analogy between an induction machine with distributed parameters and that with a double squirrel-cage rotor. In a double squirrel-cage machine, there is a rotor leakage flux that links the circuits of the upper and lower cages. The common inductive reactance corresponds to this flux. With a common end ring for both cages, there is also a common resistance. The impedances, eqns. 25 and 27 and $Z'^{(i-1)}_{vi-1}(s_v)$ should be connected together in accordance with eqns. 21. Equivalent circuits of a multilayer rotor induction machine for the vth space harmonic (without the primary winding impedances) are shown in Fig. 2.

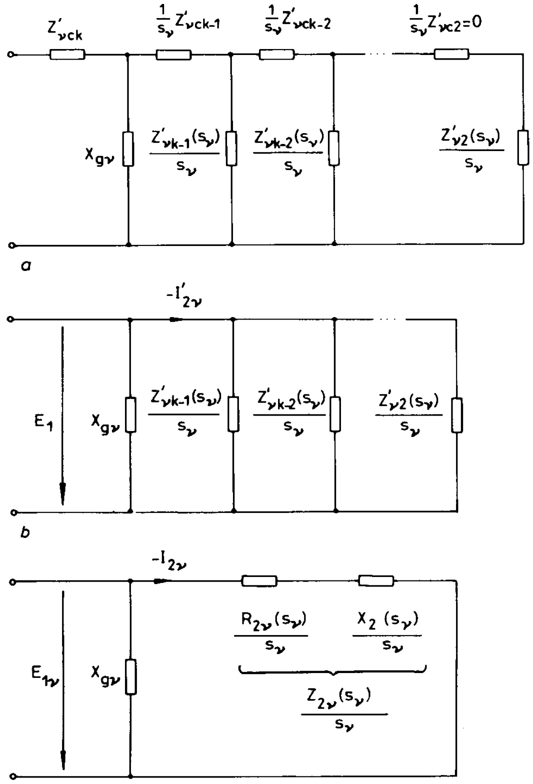

Fig. 2 *Circuit models for multilayer rotor with distributed parameters*
a Complete circuit model with common impedances
b Model without common impedances
c Model containing resultant rotor impedance

The circuit shown in Fig. 2*a* corresponds to the equivalent circuit of a multicage rotor induction motor.

In case of a rotor (secondary) with distributed parameters

$$Z'_{vci} \ll Z'^{(i)}_{vi}(s_v) \quad (28)$$

i.e. the common impedances Z_{vci} can be neglected (Appendix 9.4). In this way, the equivalent circuit of Fig. 2*a* can be simplified to that shown in Fig. 2*b*. It is a parallel circuit of k branches connected across a voltage $s_v E_v$, where E_v is the EMF induced in the stator (primary) winding. Without doubt, this equivalent circuit can be used both in practical calculations and theoretical considerations. If we denote the equivalent impedance of the rotor (secondary) by $Z'_{2v}(s_v) = Z'^{(k-1)}_{vk-1}$, the reciprocal of $Z'_{2v}(s_v)$ fulfills the following relationship:

$$\frac{1}{Z'_{2v}(s_v)} = \frac{1}{Z'_{vk-1}(s_v)} + \frac{1}{Z'_{vk-2}(s_v)} + \cdots + \frac{1}{Z'_{vi}(s_v)} + \cdots + \frac{1}{Z'_{v1}(s_v)} \quad (29)$$

The rotor current I'_{2v}, reduced to the stator circuit, is determined by the EMF E_v and the equivalent impedance of the rotor circuit as follows:

$$I'_{2v} = s_v E_v / Z'_{2v}(s_v) = \frac{E_v}{R'_{2v}(s_v)/s_v + jX'_{2v}(s_v)/s_v} \quad (30)$$

where $R'_{2v}(s_v) = \text{Re}\,[Z'_{2v}(s_v)]$ and $X'_{2v}(s_v) = \text{Im}\,[Z'_{2v}(s_v)]$ are the equivalent resistance and reactance of the rotor. Eqns. 29 and 30 allow us to modify the equivalent circuit shown in Fig. 2*b* to that of Fig. 2*c*.

5 Equivalent circuit for induction motor under unbalanced conditions

In the case of an unbalanced system of the input currents and no neutral wire, the result of the symmetrical components theory is that

$$\begin{aligned} I^{+}_{1v} &= \tfrac{1}{3}(I_{1A} + a^v I_{1B} + a^{2v} I_{1C}) \\ I^{-}_{1v} &= \tfrac{1}{3}(I_{1A} + a^{2v} I_{1B} + a^v I_{1C}) \\ I^{0}_{1v} &= \tfrac{1}{3}(I_{1A} + I_{1B} + I_{1C}) = 0 \end{aligned} \quad (31)$$

where I^{+}_{1v} = positive-sequence current, I^{-}_{1v} = negative-sequence current, I^{0}_{1v} = zero-sequence current, $a = \exp(2j\pi/3)$ and I_{1A}, I_{1B}, I_{1C} = phase stator currents, expressed in phasor terms. The positive-sequence currents I^{+}_{1v} and negative-sequence currents I^{-}_{1v} are discussed in Appendix 9.5.

The equivalent circuits for positive-sequence and negative-sequence components are presented in Fig. 3. According to Reference 20, any induction motor can be represented by a series of mechanically connected motors having a different number $2vp$ of poles the stator windings of which are connected in series. The impedance of the stator winding is taken into account during consideration of the winding resistances and leakage reactances of the slots and end connections. Any vth rotor is characterised by a mutual inductance representing the self-inductance reactance X_{gv}. The coefficient of coupling between the stator and the rotor for $v > 1$ is assumed to be equal to 1. The impedance of the vth rotor referred to the stator is Z'_{2v}, where the real part represents its resistance and the imaginary part represents its leakage reactance.

The slip corresponding to higher space harmonics (Fig. 3) is expressed by formula 4*a* if $v = 1, 7, 13, \ldots$ (positive sequence) and $v = 5, 11, 17, \ldots$ (negative sequence). The slip is expressed by formula 4*b* if $v = 5, 11, 17, \ldots$ (positive sequence) and $v = 1, 7, 13, \ldots$ (negative sequence). For the negative-sequence components, the forward-travelling magnetic field moves backwards.

For a balanced current system, i.e. $|I_{1A}| = |I_{1B}| = |I_{1C}|$, the positive-sequence component $I^{+}_{1v} = |I_1|$ and the negative-sequence component $I^{-}_{1v} = 0$. This makes the branch *b* of the equivalent circuit shown in Fig. 3 vanish.

The equivalent circuit of Fig. 3 may be also helpful in the analysis of the longitudinal end effect in a linear

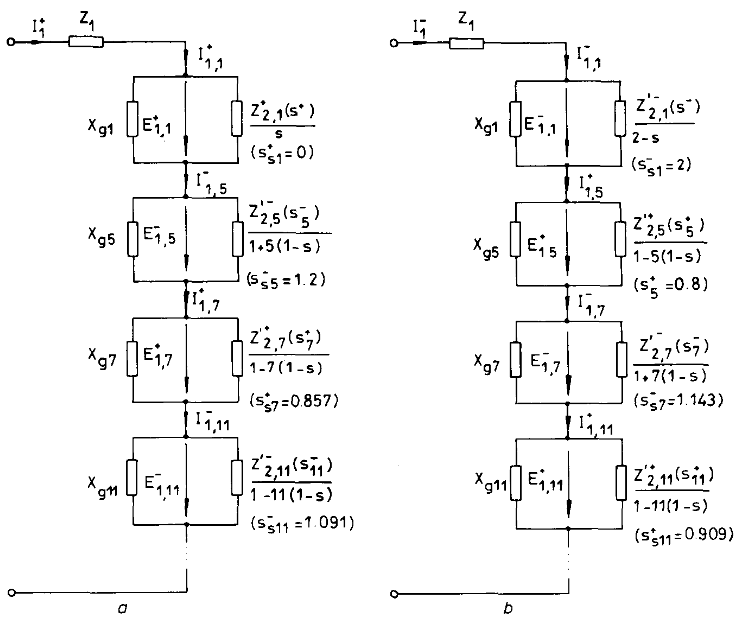

Fig. 3 *Equivalent circuits for multilayer rotor induction motor under unbalanced conditions*
a For positive-sequence current
b For negative-sequence current

induction motor. The unbalanced currents in linear induction motors are among those caused by this effect.

The slip corresponding to a synchronous speed $n_{s\nu}$ (in rev/min) or $v_{s\nu}$ (in m/s) can be determined by understanding that the pole pitch τ_ν for the νth space harmonic is ν times smaller than the pole pitch τ for the fundamental, i.e.

$$\tau = \tau/\nu \tag{32}$$

$$|n_{s\nu}| = n_s/\nu \tag{33a}$$

$$|v_s| = v_s/\nu \tag{33b}$$

where n_s and v_s = synchronous speed for $\nu = 1$. Hence

$$s_{s\nu} = 1 \pm \frac{1}{\nu} \tag{34}$$

In the case of positive-sequence components $I_{1,1}^+ = I_{1,5}^- = I_{1,7}^+ = \cdots = I_1^+$, the '−' sign ($s_{s\nu} < 1$, $n_{s\nu} > 0$) is for $\nu = 1, 7, 13, \ldots$ and the '+' sign ($s_{s\nu} > 1$, $n_{s\nu} < 1$) is for $\nu = 5, 11, 17, \ldots$. In the case of negative-sequence components $I_{1,1}^- = I_{1,5}^+ = I_{1,7}^- = \cdots = I_1^-$, the '−' sign is for $\nu = 5, 11, 17, \ldots$, and the '+' sign is for $\nu = 1, 7, 13, \ldots$. If $\nu \to \infty$ then $s_{s\nu} \to 1$.

6 Performance

To calculate the performance characteristics of a multilayer rotor induction motor under unbalanced conditions, it is necessary to find the airgap induced voltages (EMFs) $|E_{1\nu}^+|$ and $|E_{1\nu}^-|$ and the airgap powers $P_{g\nu}^+$ and $P_{g\nu}^-$ for each of the space harmonics separately. The RMS EMFs

$$|E_{1\nu}^+| = |I_{1\nu}^+||Z_{t\nu}^+| \tag{35a}$$

$$|E_{1\nu}^-| = |I_{1\nu}^-||Z_{t\nu}^-| \tag{35b}$$

can be calculated as voltage drops across the impedance

$$Z_{t\nu} = \frac{jX_{g\nu} Z'_{2\nu}(s_\nu)}{Z'_{2\nu}(s_\nu) + jX_{g\nu}(s_\nu)} \tag{36}$$

The resistance $R'_{2\nu}(s_\nu)/s_\nu$ absorbs the total power crossing the airgap, i.e.

$$P_{g\nu}^+ = m_1(|I'^+_{2\nu}|)^2 R'^+_{2\nu}(s_\nu^+)/s_\nu^+ \tag{37a}$$

$$P_{g\nu}^- = m_1(|I'^-_{2\nu}|)^2 R'^-_{2\nu}(s_\nu^-)/s_\nu^- \tag{37b}$$

where the rotor RMS currents $|I'^+_{2\nu}|$ and $|I'^-_{2\nu}|$ are expressed by eqn. 30. If the airgap powers are known, the forces

$$F_{d\nu}^+ = P_{g\nu}^+/v_{s\nu}^+ \tag{38a}$$

$$F_{d\nu}^- = P_{g\nu}^-/v_{s\nu}^- \tag{38b}$$

and torques

$$T_{d\nu}^+ = P_{g\nu}^+/(2\pi n_{s\nu}^+) \tag{39a}$$

$$T_{d\nu}^- = P_{g\nu}^-/(2\pi n_{s\nu}^-) \tag{39b}$$

developed by the electromagnetic energy conversion process can be found.

The forces (eqns. 38*a* and *b*) or torques (eqns. 39*a* and *b*) are positive or negative since the airgap powers (eqns. 37*a* and *b*) are dependent on slip, which can be positive or negative.

The resultant developed force and torque

$$F_d = \sum_\nu (F_{d\nu}^+ + F_{d\nu}^-) \tag{40}$$

$$T_d = \sum_\nu (T_{d\nu}^+ + T_{d\nu}^-) \tag{41}$$

Fig. 4 shows the torques $T_{d\nu}^+$ and $T_{d\nu}^-$ as functions of slip for $\nu = 1, 5$ and 7.

7 Conclusions

A field analysis is shown to be capable of accurately modelling the induction machines with distributed parameters. Considerations presented here can be helpful in the analysis and synthesis of induction machinery with specially constructed rotors (secondaries).

The multiregion problem in induction machines, discussed here, is the general case for a wide variety of special cases, e.g. solid rotor induction motors, induction

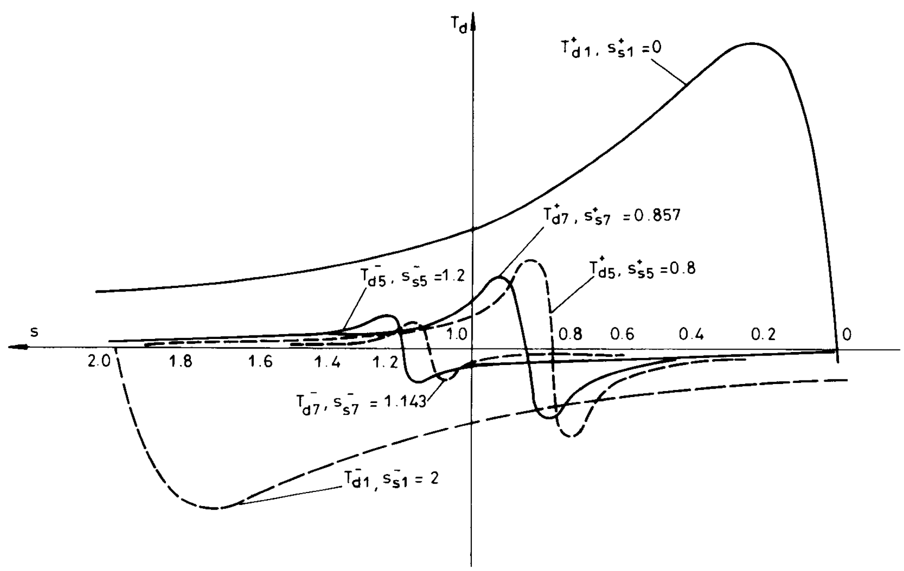

Fig. 4 *Torque-slip curves for higher time harmonics $\nu = 1, 5$ and 7*

motors with screened rotors, low-inertia servo motors, linear induction motors, eddy-current brakes and couplings, magnetic levitation devices etc. The field theory allows us to develop an equivalent circuit for any induction machine. In the case of a rotor with distributed parameters, the field theory is equivalent to the circuit theory. The electromagnetic field equations determine both the impedance of the rotor and the impedance of the airgap. This paper shows how to separate the impedance for each layer, and the self-inductance reactance, and how to determine the differential leakage reactance.

The equivalent circuit for a multilayer rotor induction motor can be easily adjusted for the analysis of a single-sided linear induction motor by including the longitudinal end effect impedance [21, 22].

To calculate the performance of various kinds of induction machines with distributed parameters, a general computer program can be constructed.

8 References

1 PIPES, L.A.: 'Matrix theory of skin effect in laminations', *J. Franklin Inst.*, 1956, **262**, (2), pp. 127–138

2 GREIG, J., and FREEMAN, E.M.: 'Travelling-wave problem in electrical machines', *Proc. IEE*, 1967, **114**, (11), pp. 1681–1683

3 FREEMAN, E.M.: 'Travelling waves in induction machines: input impedance and equivalent circuits', *ibid.*, 1968, **115**, (12), pp. 1172–1176

4 FREEMAN, E.M., and SMITH, B.E.: 'Surface-impedance method applied to multilayer cylindrical induction devices with circumferential exciting currents', *ibid.*, 1970, **117**, (10), pp. 2012–2013

5 FREEMAN, E.M.: 'Equivalent circuits from electromagnetic theory: low frequency induction devices', *ibid.*, 1974, **121**, (10), pp. 1117–1121

6 FREEMAN, E.M.: 'Computer-aided steady-state and transient solutions of field problems in induction devices', *ibid.*, 1977, **124**, (11), pp. 1057–1061

7 CULLEN, A.L., and BARTON, C.H.: 'A simplified electromagnetic theory of induction motor, using the concept of wave impedance', *ibid.*, 1958, **105C**, (8), pp. 331–336, Monograph 283U

8 WILLIAMSON, S.: 'The anisotropic layer theory of induction machines and induction devices', *J. Inst. Math. & Appl.*, 1976, **17**, (2), pp. 69–84

9 RIEPE, F.: 'Zweidimensionaler rechnergestützter Entwurf von Drehstrom-Asynchronmachinen mit massiven Läufern', *ETZ Arch.*, 1981, **3**, (2), pp. 71–75

10 BOLDEA, I., and BABESCU, M.: 'Multilayer theory of DC linear brakes with solid-iron secondary', *Proc. IEE*, 1976, **123**, (3), pp. 220–222

11 BOLDEA, I., and BABESCU, M.: 'Multilayer approach to the analysis of single-sided linear induction motors', *ibid.*, 1978, **125**, (4), pp. 283–287

12 BRATOLJIC, T.: 'Negative sequence and eddy current losses in the rotor of a superconducting turboalternator'. Sixth International Conference on Magnet Technology MT6, Bratislava, Czechoslovakia, 1977, pp. 206–211

13 GIERAS, J.F.: 'General equations of electromagnetic field distribution in composite multilayer structures for one-sided wave penetration', *Acta Tech. CSAV*, 1977, **22**, (5), pp. 361–386

14 GIERAS, J.F.: 'Elements of electromagnetic theory of induction machines'. DSc Thesis, *Zesz. Nauk. ATR Elektrotechnika*, Bydgoszcz, Poland, 1979, **70**, (2), in Polish

15 GIERAS, J.F.: 'Three dimensional multilayer theory of induction machines and devices', *Acta Tech. CSAV*, 1983, **28**, (5), pp. 525–548

16 WAIT, J.R.: 'Electromagnetic surface impedance for a layered earth for general excitation', *Radio Sci.*, 1980, **15**, pp. 129–134

17 GIERAS, J.F.: 'Analytical method of calculating the electromagnetic field and power losses in ferromagnetic halfspace, taking into account saturation and hysteresis', *Proc. IEE*, 1977, **124**, (11), pp. 1098–1104

18 RUSSELL, R.L., and NORSWORTHY, K.M.: 'Eddy currents and wall losses in screened rotor induction motors', *ibid.*, 1958, **105A**, pp. 163–175

19 YEE, H.: 'Effects of finte length in solid-rotor induction machines', *ibid.*, 1971, **118**, (8), pp. 1025–1033

20 HELLER, B., and HAMATA, V.: 'Harmonic field effects in induction machines' (Academia, Prague, Czechoslovakia, 1977)

21 GIERAS, J.F., DAWSON, G.E., and EASTHAM, A.R.: 'A new longitudinal end effect factor for linear induction motors'. IEEE Trans. 1987, **EC-2**, (1), pp. 152–159

22 GIERAS, J.F., DAWSON, G.E., and EASTHAM, A.R.: 'Performance calculation for single-sided linear induction motor with double-layer reaction rail under constant current excitation'. IEE Trans., 1986, **MAG-22**, (1), pp. 54–62

23 MARSHALL, S.V., and SKITEK, G.G.: 'Electromagnetic concepts and applications' (Prentice-Hall Inc., Englewood Cliffs, New Jersey, USA, 1987)

9 Appendixes

9.1 Boundary conditions

The magnetic field distribution at the boundary $z = 0$ can be found on the basis of

(*a*) Ampère's circuital law and an amperian closed path (non-salient-pole machines):

$$H_{xvk}^{(k)+}(x, 0, t) = -A_v^+ \exp\left[j(\omega s_{vi}^+ t - \beta_v x)\right]$$
$$H_{xvk}^{(k)-}(x, 0, t) = -A_v^- \exp\left[j(\omega s_{vi}^- t + \beta_v x)\right] \quad (42)$$

(*b*) the equality of normal components of magnetic flux (salient-pole machines)

$$\mu_0 H_{zvk}^{(k)+}(x, 0, t) = B_v^+ \exp\left[j(\omega s_{vi}^+ t - \beta_v x)\right]$$
$$\mu_0 H_{zvk}^{(k)-}(x, 0, t) = B_v^- \exp\left[j(\omega s_{vi}^- t + \beta_v x)\right] \quad (43)$$

where A_v^+ and A_v^- = peak values of the vth harmonics of the stator line current density and B_v^+ and B_v^- = peak values of the vth harmonics of the airgap magnetic flux density (normal components).

The application of other boundary conditions yields

(i) $z = d_k$

$$H_{xvk}^{(k)}(x, d_k, t) = H_{xvk-1}^{(k)}(x, d_k, t)$$
$$\mu_k H_{zvk}^{(k)}(x, d_k, t) = \mu_{k-1} H_{zvk-1}^{(k)}(x, d_k, t) \quad (44)$$

(ii) $z = \sum_{i=k-1}^{k} d_i$

$$H_{xvk-1}^{(k)}\left(x, \sum_{i=k-1}^{k} d_i, t\right) = H_{xvk-2}^{(k)}\left(x, \sum_{i=k-1}^{k} d_i, t\right)$$
$$\mu_{k-1} H_{zvk-1}^{(k)}\left(x, \sum_{i=k-1}^{k} d_i, t\right) = \mu_{k-2} H_{zvk-2}^{(k)}\left(x, \sum_{i=k-1}^{k} d_i, t\right) \quad (45)$$

....

(iii) $z = \sum_{i=2}^{k} d_i$

$$H_{xv2}^{(k)}\left(x, \sum_{i=2}^{k} d_i, t\right) = H_{xv1}^{(k)}\left(x, \sum_{i=2}^{k} d_i, t\right)$$
$$\mu_2 H_{zv2}^{(k)}\left(x, \sum_{i=2}^{k} d_i, t\right) = \mu_1 H_{zv1}^{(k)}\left(x, \sum_{i=2}^{k} d_i, t\right) \quad (46)$$

Moreover, for $z \to \infty$ $C_{1v1}^{(k)} C_{4v1}^{(k)} = C_{2v1}^{(k)} C_{4v1}^{(k)} = 0$. Eqns. 42 and 44–46 or 43 and 44–46 allow to find all the constants $C_{1vi}^{(k)}$, $C_{2vi}^{(k)}$, $C_{3vi}^{(k)}$ and $C_{4vi}^{(k)}$. Some details are given in the references [13–15].

9.2 Analogy to transmission line

If we let $z_{0v}^{(i)} = j\omega_{vi}\mu_i/x_{vi}$ and $z_{Lv}^{(i-1)} = (\omega_{vi}/\omega_{vi-1})z_{vi-1}^{(i-1)}$, eqn. 12*b* has the same form as that expressing the input impedance $z_{inv}^{(i)}$ of a transmission line [23] at a distance d_i from the load, i.e.

$$z_{inv}^{(i)} = z_{0v}^{(i)} \frac{z_{Lv}^{(i-1)} + z_{0v}^{(i)} \tanh(\kappa_{vi} d_i)}{z_{0v}^{(i)} + z_{Lv}^{(i-1)} \tanh(\kappa_{vi} d_i)} = \frac{\dfrac{z_{0v}^{(i)} z_{Lv}^{(i-1)}}{\tanh(\kappa_{vi} d_i)} + [z_{0v}^{(i)}]^2}{\dfrac{z_{0v}^{(i)}}{\tanh(\kappa_{vi} d_i)} + z_{Lv}^{(i-1)}} \quad (47)$$

where $z_{0v}^{(i)}$ = characteristic impedance of the line, $z_{Lv}^{(i-1)}$ = load impedance.

The characteristic impedance, by anaology to electromagnetic wave propagation, is referred to as the propagation constant divided by the electric conductivity, i.e.

$$z_{0v}^{(i)} = \frac{j\omega_{vi}\mu_i}{\kappa_{vi}} = \frac{\alpha_{vi}^2}{\sigma'\kappa_{vi}} \simeq \frac{\alpha_{vi}}{\sigma'} \simeq \frac{\kappa_{vi}}{\sigma'} \tag{48}$$

If $z_{Lv}^{(i-1)} \to \infty$ is substituted, eqn. 47 gives the input impedance of an open-circuited line [23]:

$$z_{inv\infty}^{(i)} = \frac{z_{0v}^{(i)}}{\tanh(\kappa_{vi} d_i)} \tag{49}$$

and if $z_{Lv}^{(i-1)} = 0$ is substituted, we get the input impedance of a shorted line [23]:

$$z_{invsh}^{(i)} = z_{0v}^{(i)} \tanh(\kappa_{vi} d_i) \tag{50}$$

9.3 Rotor impedance estimation

As an example, a double-layer low-inertia rotor with distributed parameters, as shown in Fig. 5, has been considered. In fact, the impedance of the copper layer and the impedance of the solid steel ring contribute only to the equivalent impedance of the rotor, which is given by eqn. 29.

Eqn. 25 allows us to estimate the impedance of the copper layer

$$Z'_{vCu}(s_v) = \frac{js_v\omega\mu_0}{\kappa_{vCu}} \frac{1}{\tanh(\kappa_{vCu} d)} k_{trv} v \frac{w}{\tau} \tag{51}$$

and the impedance of the solid steel ring (core)

$$Z'_{vFe}(s_v) = \frac{js_v\omega\mu_{Fe}}{\kappa_{vFe}} \frac{1}{\tanh(\kappa_{vFe} h_{Fe})} k_{zv} k_{trv} v \frac{w}{\tau} \tag{52}$$

where μ_{Fe} is given by eqn. 5, χ_{vFe} and χ_{vCu} are given by eqn. 9, k_{trv} is given by eqn. 20 and k_{zv} is given by eqn. 26.

The electrical conductivity of the steel cylinder is σ_{Fe}, and the electrical conductivity of the copper layer is $\sigma'_{Cuv} = k_{tev}\sigma_{Cu}$, where $k_{tev} < 1$ is the Russell and Norsworthy correction factor, used for the edge effect in the high conductivity nonmagnetic layer, i.e.

$$k_{tev} = 1 - \frac{\tanh\left(\beta_v \frac{w}{2}\right)}{\beta_v \frac{w}{2}\left[1 + k_t \tanh\left(\beta_v \frac{w}{2}\right)\tanh(\beta_v w_{0v})\right]} \tag{53}$$

in which

$$k_t = 1 + 1.3(t_{0v} - d)/d \tag{54}$$

The tranverse edge effect in the solid steel ring has been included in correction factor k_{zv}, see eqn. 26.

Similar equations to 51 and 52 are valid for the impedance of a single-sided linear induction motor (high conductivity cap over solid back iron)[22].

9.4 Simplification of equivalent circuit

The second term $(j\omega_{vi}\mu_i/\kappa_{vi})^2$ in the numerator of eqn. 15 is z_{vi} squared when $d_i \to \infty$. By taking the limit of eqn. 14 as $d_i \to \infty$, we obtain the unit impedance $z_{vi} = j\omega_{vi}\mu_i/\kappa_{vi}$ of a halfspace. The impedance of a halfspace to the second power, divided by $z_{vi} + (\omega_{vi}/\omega_{vi-1})z_{vi-1}^{(i-1)}$ must be much smaller than that of parallel-connected of layers with finite thicknesses. Hence, $(j\omega_{vi}\mu_i/\kappa_{vi}) \ll z_{vi}(\omega_{vi}/\omega_{vi-1})z_{vi-1}^{(i-1)}$. It can be visualised by considering an induction motor with for example, $\tau = 0.05$ m, $k_C k_{sat} g = 0.001$ m, $X_g = 100\,\Omega$ and $Z'_2/s = (2/s + j3)\,\Omega$. For an induction motor, $(\omega_{vi}\mu_i/\beta_v) \propto X_{gv} \tanh(\beta_v k_C k_{sat} g) \simeq X_{gv}\beta_v k_C k_{sat} g$. If $v = 1$, the product $X_g \beta k_C k_{sat} g = 100\pi$, $0.001/0.05 = 6.28\,\Omega$. For a rotor under short circuit conditions, impedance $Z'_2/s = (2 + j3)\,\Omega$, ratio $X_g\beta k_C k_{sat} g/|Z'_2| = 1.74$ and product $X_g|Z'_2| = 360\,\Omega^2$. Now, $(X_g\beta k_C k_{sat} g)^2 = 39.4\,\Omega^2$ is much smaller than $X_g|Z'_2|$. If $s = 0.03$, $X_g|Z'_2| = 6673.4\,\Omega^2$.

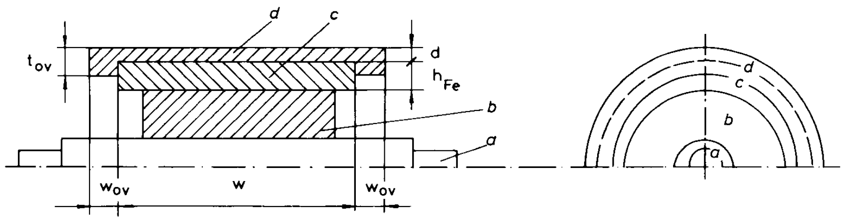

Fig. 5 *Double-layer low-inertia rotor with distributed parameters*
a Steel shaft
b Epoxide resin bush
c Steel ring
d Copper cap

With the application of the concept of transmission line, the eqn. 16 yields

$$\frac{(j\omega_{vi}\mu_i/x_{vi})^2}{z_{vi} + (\omega_{vi}/\omega_{vi-1})z_{vi-1}^{(i-1)}} = \frac{[z_{0v}^{(i)}]^2}{z_{0v}^{(i)}/\tanh(\kappa_{vi}d_i) + z_{Lv}^{(i-1)}} = \frac{z_{0v}^{(i)} z_{Lv}^{(i-1)}/\tanh(\kappa_{vi}d_i)}{z_{0v}^{(i)}/\tanh(\kappa_{vi}d_i) + z_{Lv}^{(i-1)}} \frac{z_{invsh}^{(i)}}{z_{Lv}^{(i-1)}} \tag{55}$$

Since the input impedance of a shorted line (eqn. 50) is very small, and, divided by the load impedance $z_{Lv}^{(i-1)}$, becomes much smaller, the value given by eqn. 55 is negligibly small.

9.5 Positive and negative sequence currents for u > 1

The phase currents in the phasor terms (eqn. 31) are

$$I_{1A} = |I_{1A}|\angle\beta_A, \; I_{1B} = |I_{1B}|\angle\beta_B$$

$$I_{1C} = |I_{1C}|\angle\beta|, \; |I_{1A}|, |I_{1B}|, |I_{1C}| = \text{RMS}$$

phase currents. If there is no is neutral wire, the zero-sequence current $I_{1v}^0 = 0$.

For $v = 2m_1 \; k + 1$, where $k = 0, 1, 2, 3, \ldots$, the complex factors $a^v = a$ and $a^{2v} = a^2$, for $2m_1k - 1$, where $k = 1, 2, 3, \ldots$, the complex factor $a^v = a^2$ and $a^{2v} = a$ and for $v = 2m_1k + 3$, where $k = 0, 1, 2, 3, \ldots$, $a^v = a^3 = 1$.

In the case of unequal phase currents $I_{1A} \neq I_{1B} \neq I_{1C}$, the following equalities arise

$$I_{1,1}^{+} = I_{1,5}^{-} = I_{1,7}^{+} = I_{1,11}^{-} = \cdots = I_{1}^{+} \quad (56)$$

$$I_{1,1}^{-} = I_{1,5}^{+} = I_{1,7}^{-} = I_{1,11}^{+} = \cdots = I_{1}^{-} \quad (57)$$

In the case of a balanced system, i.e. $|I_{1A}| = |I_{1B}| = |I_{1C}| = |I_1|$, $\beta_A = 0$, $\beta_B = 120°$ and $\beta_C = 240°$, the positive- and negative-sequence currents are equal to RMS phase current I_1, i.e.

(i) for $v = 6k + 1$

$$\begin{aligned} I_{1,1}^{+} &= I_{1,7}^{+} = I_{1,13}^{+} = \cdots = |I_1| \\ I_{1,1}^{-} &= I_{1,7}^{-} = I_{1,13}^{-} = \cdots = 0 \end{aligned} \quad (58)$$

(ii) for $v = 6k - 1$

$$\begin{aligned} I_{1,5}^{+} &= I_{1,11}^{+} = I_{1,17}^{+} = \cdots = 0 \\ I_{1,5}^{-} &= I_{1,11}^{-} = I_{1,17}^{-} = \cdots = |I_1| \end{aligned} \quad (59)$$